nature communications

Article

https://doi.org/10.1038/s41467-025-56752-7

Natural variation of *OsWRKY23* drives difference in nitrate use efficiency between *indica* and *japonica* rice

Received: 25 September 2024

Accepted: 30 January 2025

Published online: 06 February 2025

Check for updates

Siyu Zhang[1,5], Zhe Ji[2,5], Wu Jiao[1,5], Chengbo Shen[1], Yaojun Qin[1], Yunzhi Huang[1], Menghan Huang[1], Shuming Kang[1], Xuan Liu[1], Shunqi Li[1], Zulong Mo[1], Ying Yu[1], Bingyu Jiang[1], Yanan Tian[1], Longfei Wang[1], Qingxin Song[1], Shaokui Wang[3] & Shan Li[1,4]

Between the two major rice subspecies, *indica* varieties generally exhibit higher nitrate (NO_3^-) uptake and nitrogen (N)-use efficiency (NUE) than *japonica* varieties. Introducing efficient NO_3^- utilization alleles from *indica* into *japonica* could improve NUE, and at the same time uncover unknown regulators of NO_3^- metabolism. Here, we identify OsWRKY23 as a key regulator of NO_3^- uptake and NUE differences between *indica* and *japonica* rice. The *OsWRKY23*^{indica} allele exhibits reduced transcriptional activation of a negative regulator of auxin accumulation, *DULL NITROGEN RESPONSE1* (*DNR1*). The resultant increase in auxin level improves NO_3^- uptake and assimilation, which ultimately enhances grain yield. Geographical and evolutionary analyses reveal overlapping distribution of *OsWRKY23*^{indica} and *DNR1*^{indica}, particularly in low-fertility soils, suggesting their involvement in the adaptation to low N conditions to improve NUE and grain yield. Incorporating the OsWRKY23-DNR1 module from *indica* rice represents a promising strategy to enhance *japonica* NUE, which is crucial for sustainable agriculture.

The widespread application of nitrogen (N) fertilizers has catalyzed a remarkable surge in global crop productivity over the past five decades[1–4]. Excess N input, however, leads to increased economic costs, significant environmental damage, biodiversity loss, and health risks to human[1,2,4]. Thus, developing improved crop varieties marrying high yields with enhanced N-use efficiency (NUE) emerges as a pressing goal, pivotal for steering agriculture towards greater sustainability while curbing N demand. Rice (*Oryza sativa* L.) is one of the most important staple crops globally, serving as the primary food source for over half of the world's population[3]. Nitrate (NO_3^-) represents one of the major sources of N for rice, even when grown under anerobic paddy field conditions due to significant nitrification in the rhizosphere[5,6]. Interestingly, the two primary subspecies of Asian cultivated rice, *indica*, and *japonica*, differ in their NUE, with *indica* varieties generally exhibiting superior NO_3^- absorption activity and NO_3^- assimilation capacity compared to *japonica* varieties[5]. Therefore, deciphering the molecular mechanisms underlying this difference is likely to allow the discovery of regulators of NO_3^- metabolism and provide strategies to improve NUE not only in *japonica* rice but also in other crops.

To date, natural allelic variations of five genes in *indica* and *japonica* subspecies of rice have been identified that contribute to their difference in NO_3^- uptake and assimilation. First, the *indica* variant of the NO_3^- transporter-encoding *OsNRT1.1B* has been associated with increased NO_3^- uptake and root-to-shoot transport, resulting in significantly enhanced grain yield and NUE compared to the *japonica*

[1]State Key Laboratory of Crop Genetics & Germplasm Enhancement and Utilization, Nanjing Agricultural University, Nanjing, China. [2]Department of Biology, University of Oxford, Oxford, UK. [3]State Key Laboratory for Conservation and Utilization of Subtropical Agro-Bioresources, South China Agricultural University, Guangzhou, China. [4]Jiangsu Collaborative Innovation Center for Modern Crop Production, Nanjing Agricultural University, Nanjing, China. [5]These authors contributed equally: Siyu Zhang, Zhe Ji, Wu Jiao. e-mail: shanli@njau.edu.cn

OsNRT1.1B allele[5]. Second, the *indica* and *japonica* variants of the NO_3^- reductase (NR) protein OsNR2 differ in one amino acid within the NAD(P) binding domain, which results in *indica* OsNR2 conferring greater NR activity[7]. Therefore, rice varieties harboring the *indica OsNR2* allele exhibit superior grain yield and NUE relative to those with *japonica OsNR2*, which is also partially attributed to a feed-forward interaction with OsNRT1.1B[5,7]. Third, a recent quantitative trait loci analysis revealed that the allelic variation of *MYB61*, encoding a crucial transcriptional regulator of cellulose synthesis downstream of the NUE-regulating GROWTH-REGULATING FACTOR4 (GRF4), contributes to the difference in NUE between the two rice subspecies[8]. Specifically, the *indica MYB61* allele leads to a higher expression level, which enhances NUE and grain yield, particularly under conditions of low N availability, through a yet unresolved mechanism. Finally, accumulating evidence highlights a pivotal role played by auxin in governing rice NUE, with two genes encoding negative regulators of auxin abundance, *REGULATOR OF N-RESPONSIVE RSA ON CHROMOSOME 10* (*RNR10*) and *DULL NITROGEN RESPONSE1* (*DNR1*), displaying allelic differences between *indica* and *japonica* varieties[9,10]. DNR1 is an aminotransferase that catalyzes the conversion of indole-3-pyruvate to L-Trp, the opposite reaction in the auxin biosynthetic pathway, thereby repressing auxin accumulation[9]. RNR10 serves as an F-box protein that stabilizes DNR1 through monoubiquitination[10]. The *indica* variants of both *RNR10* and *DNR1* lead to reduced transcript and protein abundances, and the resultant elevation in auxin level enhances NO_3^- uptake, NO_3^- assimilation, and N-responsive reshaping of root architecture. Indeed, knocking out *RNR10* or *DNR1* in *japonica* rice has been shown to improve NUE and grain yield, demonstrating the feasibility of exploiting advantageous variant genes for optimizing crop performance and therefore the need to identify additional regulatory genes that contribute to the divergent NUE between rice subspecies[9,10].

In this study, we report the isolation of a single segment substitution line (SSSL)-W56 among 82 SSSLs that exhibits reduced NO_3^- uptake, from which the OsWRKY23 transcription factor is identified as a positive regulator of *DNR1*. The $OsWRKY23^{indica}$ allele results in reduced OsWRKY23 abundance, which leads to decreased *DNR1* transcript abundance, increased auxin accumulation, and ultimately enhanced NO_3^- uptake and grain yield. These findings shed light on the intricate OsWRKY23-DNR1-auxin regulatory module involved in NUE regulation and its impact on grain yield for sustainable agriculture.

Results

OsWRKY23 is a negative regulator of rice NO_3^- uptake

To identify additional N regulator(s) responsible for the difference in NO_3^- uptake rate between *indica* and *japonica* subspecies, we crossed *indica* HJX74 (with higher NO_3^- uptake activity) as the recurrent parent and *japonica* IRAT261 (with lower NO_3^- uptake activity) as the donor parent to generate a set of 82 single segment substitution lines (SSSLs), each containing a single chromosome segment from IRAT261 substituted into the HJX74 genetic background (Supplementary Fig. 1a)[11]. Compared to HJX74, one of the SSSLs, SSSL-W56, which carries a segment from IRAT261 on the long arm of chromosome 1, exhibited a reduced NO_3^- uptake rate (Fig. 1a, b). A mapping population was generated by crossing SSSL-W56 (donor parent) and HJX74 (recurrent parent), from which positional cloning using 132 BC_1F_2 and 862 BC_2F_2 progenies narrowed down the candidate region to a ~ 4.5 kb stretch flanked by the markers WR16 and WR17 (Fig. 1c). This segment contains the promoter and partial coding region of LOC_Os01g53260, also known as *OsWRKY23* (Fig. 1c). The alignment of *OsWRKY23* genomic sequences from HJX74 and SSSL-W56 revealed several differences: 23 SNPs (single-nucleotide polymorphisms) and 13 INDELs (insertions and deletions) including a large insertion, 393-bp in the promoter region of SSSL-W56 *OsWRKY23* ($OsWRKY23^{IRAT261}$) (Supplementary Fig. 2a). Moreover, we expanded our analysis by comparing the *OsWRKY23* sequences in 12 *indica* and 12 *japonica* varieties, discovering that the 393-bp INDEL was widely conserved and specific to the rice subspecies, which likely explains the generally higher expression level of *OsWRKY23* in *japonica* compared to *indica* (Supplementary Fig. 2b, c). Additionally, we found that the transcript and protein levels of OsWRKY23 were positively regulated by external N (Fig. 1d, e).

To confirm that the allelic variation of *OsWRKY23* underlies the difference in NO_3^- uptake rate between *indica* and *japonica* varieties, we created a near-isogenic line (NIL) in the HJX74 background, containing the *japonica* allele of *OsWRKY23* from IRAT261, termed NIL-$OsWRKY23^{IRAT261}$ (Fig. 1f). Compared to the control (NIL-$OsWRKY23^{HJX74}$), NIL-$OsWRKY23^{IRAT261}$ plants displayed reduced NO_3^- uptake rate, alongside semi-dwarfism, increased tillering, and reduced panicle branching, grain number, and yield (Fig. 1g–i; Supplementary Fig. 3). These changes were attributed to elevated levels of *OsWRKY23* mRNA and protein in NIL-$OsWRKY23^{IRAT261}$ (Fig. 1j, k), suggesting that $OsWRKY23^{indica}$ is a reduced function allele associated with desirable agronomic traits. It is worth noting that these differences in aboveground phenotypes, with the exception of mature plant height, were also observed in the parental HJX74 and IRAT261 cultivars (Supplementary Fig. 1b–e), which further indicated that OsWRKY23 additionally regulates shoot phenotypes.

To further understand the phenotypic consequences of varying *OsWRKY23* expression, we constructed independent *pAct::OsWRKY23-Flag* overexpression and *oswrky23* mutant lines in the Zhonghua 11 (ZH11, a *japonica* rice variety) background (Fig. 2a). The two *oswrky23* mutants were generated by CRISPR/Cas9, which resulted in a 1-bp deletion and a 1-bp insertion in the first exon of *OsWRKY23*, respectively, both leading to an early stop codon that disrupted its normal gene function (Supplementary Fig. 4). Notably, *oswrky23* plants exhibited increased NO_3^- uptake, tall stature, reduced tiller number, increased panicle branching, grain number, and yield, whereas the exact opposite phenotypes were observed in the *pAct::OsWRKY23-Flag* overexpression lines (Fig. 2a–f; Supplementary Fig. 5). Additionally, the activity of NR mediating NO_3^- assimilation was higher in the *oswrky23* mutants and lower in the *OsWRKY23* overexpression lines (Fig. 2g). Taken together, OsWRKY23 negatively regulates both NO_3^- uptake and assimilation.

OsWRKY23 targets *DNR1* for transcriptional activation

We confirmed that OsWRKY23 functions as a transcription factor by demonstrating that transiently expressed OsWRKY23 fused with green fluorescent protein (GFP) predominantly localized in the nucleus of rice protoplasts (Supplementary Fig. 6a). Nuclear and cellular protein extracts isolated from transgenic lines (ZH11 *pAct::OsWRKY23-Flag*) indicated the presence of the OsWRKY23-Flag fusion protein only in the nuclear compartment (Fig. 3a). Further, transcription activation assays in both yeast and rice protoplast showed that OsWRKY23 possesses transcription activation activity, with the N-terminal region (1-174) being sufficient and necessary for reporter activation (Fig. 3b; Supplementary Fig. 6b).

To understand how OsWRKY23 regulates root NO_3^- uptake, we performed DNA sequencing of OsWRKY23 chromatin immunoprecipitation products (ChIP-seq), and identified *DNR1* as a downstream target gene of OsWRKY23 (Fig. 3c). ChIP-qPCR and electrophoretic mobility shift assays (EMSA) confirmed in vivo and in vitro OsWRKY23 binding to the two TTGAC/AACTG core sequence[12]-containing promoter fragments of *DNR1* (Fig. 3d, e; Supplementary Fig. 7; Supplementary Data 1), respectively. To determine which of the two core sequences within the ~3 kb promoter is important, we first compared ~25 bp sequences before and after the two TTGAC core sequences and found no difference in the sequences surrounding the TTGAC at positions -701 ~ -705. However, a single nucleotide polymorphism (SNP) was identified in the ~25 bp sequences around the TTGAC at positions -561 ~ -565, distinguishing *indica* from *japonica* rice (A in

https://doi.org/10.1038/s41467-025-56752-7

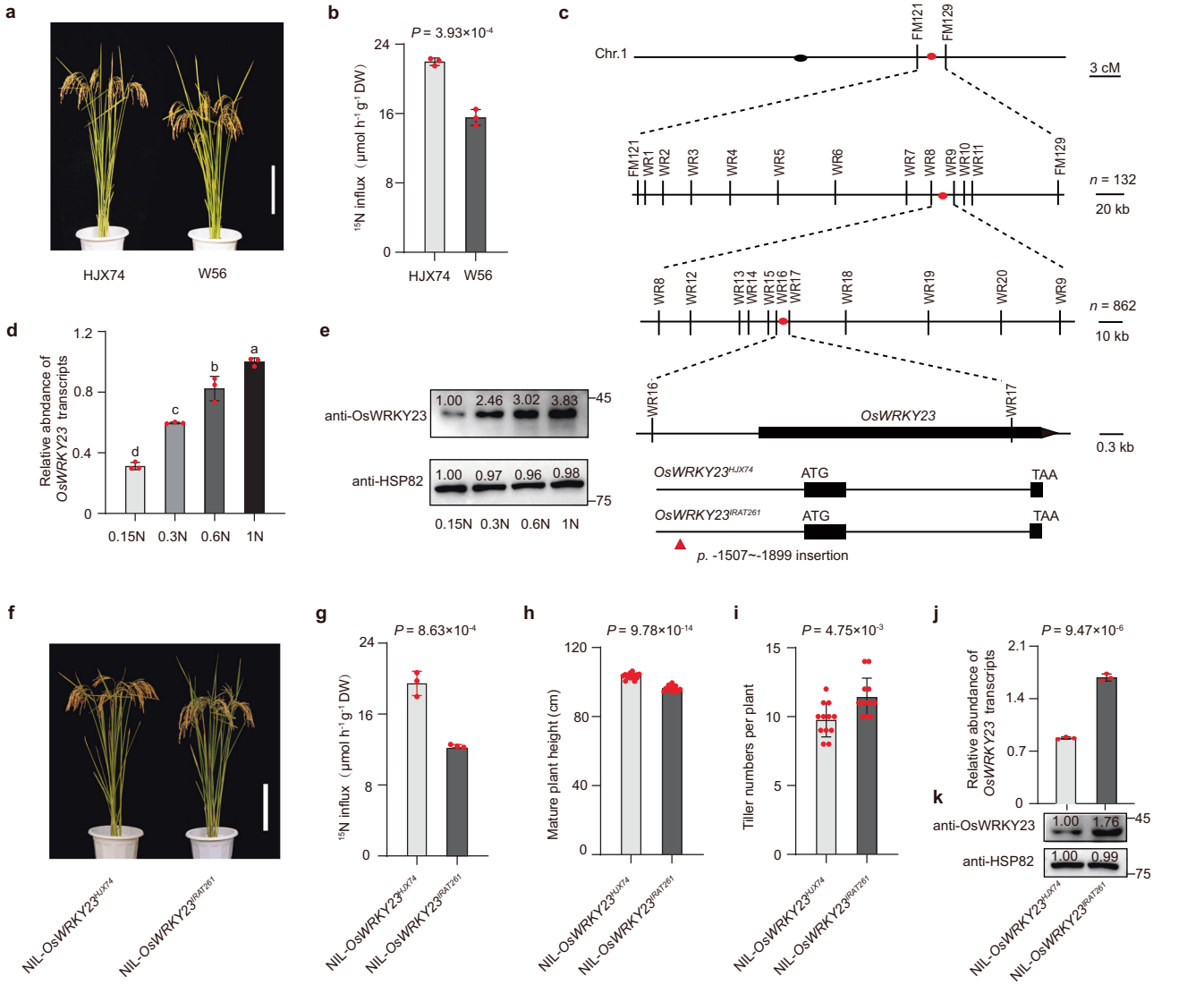

Fig. 1 | Allelic variation of *OsWRKY23* underlies the difference in NO_3^- uptake rate between *indica* and *japonica* varieties. a Morphology of HJX74 and W56 plants. Scale bar, 20 cm. **b** $^{15}NO_3^-$ uptake rates of HJX74 and W56. *P* values were generated from two-side Student's *t* tests. Data are mean ± s.e.m. ($n = 3$ biological replicates). **c** Successive maps of the candidate gene, *OsWRKY23*, using indicated recombination breakpoints and linked DNA markers to an ~ 4.5 kb segment flanked by the markers WR16 and WR17 on chromosome 1. The gene structure of *OsWRKY23* is shown underneath, where the thick black bars represent the protein-coding sequence, with the start and stop codons labeled as ATG and TAA, respectively. The 393-bp insertion in the $OsWRKY23^{IRAT261}$ promoter relative to the *OsWRKY23* start ATG (nucleotide 1), is shown as a red triangle. **d** Root *OsWRKY23* mRNA levels in HJX74 grown in nutrient solutions with different N supply (0.15 N, 0.09375 mM $(NH_4)_2SO_4$ and 0.1875 mM KNO_3; 0.3 N, 0.1875 mM $(NH_4)_2SO_4$ and 0.375 mM KNO_3; 0.6 N, 0.375 mM $(NH_4)_2SO_4$ and 0.75 mM KNO_3; 1 N, 0.625 mM $(NH_4)_2SO_4$ and 1.25 mM KNO_3). Transcript abundance was measured relative to 1 N (set to 1). Different letters denote significant differences ($P < 0.05$) from a two-side Duncan's multiple range test. Data are mean ± s.e.m. ($n = 3$ biological replicates). **e** Root OsWRKY23 protein abundance with different N supply. HSP82 severs as loading control. Data are representative of three independent experiments, with similar results. **f** Morphology of NIL-$OsWRKY23^{HJX74}$ and NIL-$OsWRKY23^{IRAT261}$. Scale bar, 20 cm. **g** $^{15}NO_3^-$ uptakes rate of NIL-$OsWRKY23^{HJX74}$ and NIL-$OsWRKY23^{IRAT261}$. The *P* value was generated from two-side Student's *t* test. Data are mean ± s.e.m. ($n = 3$ biological replicates). **h**, **i** Plant height (**h**) and the number of tillers per plant (**i**) of NIL-$OsWRKY23^{HJX74}$ and NIL-$OsWRKY23^{IRAT261}$. *P* values were generated from two-side Student's *t* tests. **h** Data are mean ± s.e.m. ($n = 16$ biological replicates). **i** Data are mean ± s.e.m. ($n = 12$ biological replicates). **j** Root *OsWRKY23* transcript abundance. Transcript abundance was measured relative to NIL-$OsWRKY23^{HJX74}$ (set to 1). The *P* value was generated from two-sided Student's *t* test. Data are mean ± s.e.m. ($n = 3$ biological replicates). **k** Root OsWRKY23 protein abundance. HSP82 severs as a loading control. Data are representative of three independent experiments, with similar results. Source data are provided as a Source Data file.

japonica rice, C in *indica* rice)[9], which did not affect the binding affinity of OsWRKY23 to the core sequences at this position in the promoters of both $DNR1^{indica}$ and $DNR1^{japonica}$ (Fig. 3e). Next, we found that OsWRKY23 exhibited no difference in binding to the two core sequences within the ~3 kb promoter region (Fig. 3e). Interestingly, yeast one-hybrid (Y1H) and rice protoplasts transient expression assays revealed that *indica* and *japonica DNR1* promoters exhibited different sensitivity to OsWRKY23 (Fig. 3f–h). Specifically, Y1H assays showed that OsWRKY23 bound more strongly to the *japonica DNR1* promoter than to the *indica DNR1* promoter, and transcriptional activation assays demonstrated that this resulted in a stronger activation of the *japonica DNR1* gene. These findings may help explain the higher expression level of *DNR1* in *japonica* rice. We have previously identified multiple SNPs in the *DNR1* promoter of *japonica* and *indica* varieties, as well as a 520-bp fragment that is only present in the *japonica DNR1* promoter[9]. We speculate that this *japonica*-specific 520-bp fragment might result in the stronger activation of *DNR1* by OsWRKY23. To test this, we compared OsWRKY23 binding and activation activities on a

https://doi.org/10.1038/s41467-025-56752-7

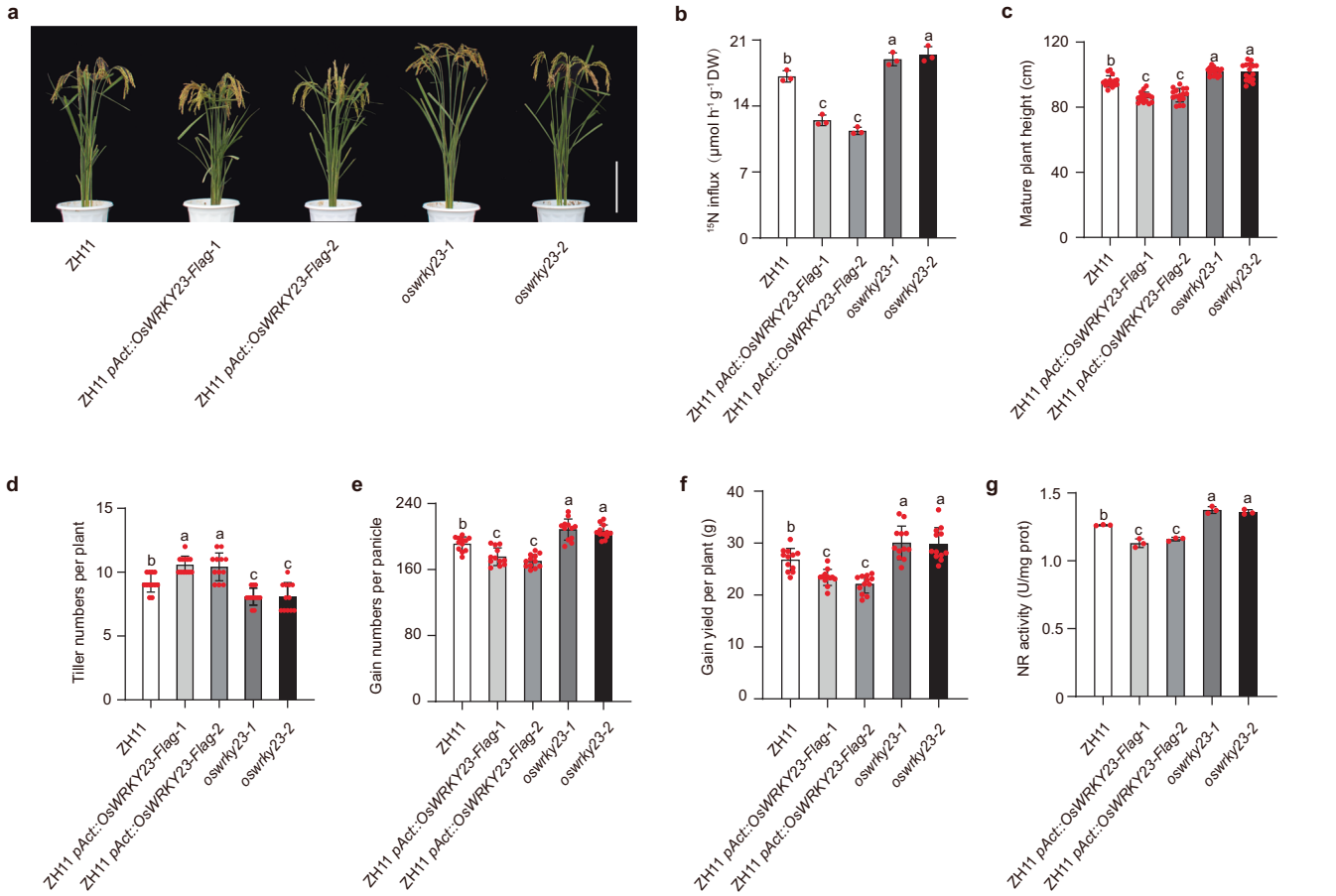

Fig. 2 | *OsWRKY23* is a negative regulator of N metabolism and grain yield. **a** Morphology of mature ZH11, ZH11/*pAct::OsWRKY23-Flag*-1, ZH11/*pAct::OsWRKY23-Flag*-2, *oswrky23*-1 and *oswrky23*-2 plants. Scale bar, 20 cm. **b**–**g** $^{15}NO_3^-$ uptake rate (**b**), plant height (**c**), the number of tillers per plant (**d**), the number of grains (**e**), grain yield per plant (**f**), and NR activity (**g**) of ZH11, ZH11/*pAct::OsWRKY23-Flag*-1, ZH11/*pAct::OsWRKY23-Flag*-2, *oswrky23*-1 and *oswrky23*-2 plants. Different letters denote significant differences ($P < 0.05$) from a two-side Duncan's multiple range test. **b**, **g** Data are mean ± s.e.m. ($n = 3$ biological replicates). **c**, Data are mean ± s.e.m. ($n = 16$ biological replicates). **d**–**f** Data are mean ± s.e.m. ($n = 12$ biological replicates). Source data are provided as a Source Data file.

native *japonica DNR1* promoter and one that has this 520-bp fragment removed, and a native *indica DNR1* promoter and one that has this fragment inserted. The results showed that this 520-bp fragment indeed determined the sensitivity of the *DNR1* promoter to OsWRKY23, with the modified *japonica DNR1* promoter less responsive to OsWRKY23 activation and vice versa for the modified *indica DNR1* promoter (Fig. 3f–h).

To further establish the regulatory role played by OsWRKY23 on *DNR1* expression, we conducted RT-qPCR and western blotting analyses, which showed that both the transcript and protein levels of DNR1 were more abundant in ZH11/*pAct::OsWRKY23-Flag* plants and less abundant in the *oswrky23* mutants, compared to the ZH11 WT control (Fig. 3i, j). This led to decreased auxin level in ZH11/*pAct::OsWRKY23-Flag* plants and increased auxin level in the *oswrky23* mutants (Fig. 3k). Since DNR1 is also responsible for regulating the size of the root system architecture (RSA)[9], we subsequently compared the RSAs among these materials and found that, compared to ZH11, *oswrky23* plants displayed larger root systems (longer total root length, greater total root area, and an increased number of roots) whereas the opposite was observed for the *OsWRKY23* overexpression lines (Supplementary Fig. 8). Finally, *OsWRKY23* was found to be predominantly expressed in the root, shoot, leaf, and node tissues, which correlated with the observed phenotypic changes in the *OsWRKY23* knockout and overexpression lines, particularly regarding root NO_3^- uptake, RSA and shoot architecture, and this expression pattern was also similar to that of *DNR1* (Supplementary Fig. 9). Collectively, these results suggested that OsWRKY23 targets *DNR1* for transcriptional activation, and thereby repressing root NO_3^- uptake and plant growth.

OsWRKY23 acts upstream of *DNR1* to regulate NO_3^- metabolism via OsARFs

Previously, we developed a NIL in the HJX74 background carrying the *japonica DNR1* allele from IRAP9, termed NIL-$DNR1^{IRAP9}$. Due to the higher activity of the *japonica DNR1* promoter, DNR1 abundance is higher in NIL-$DNR1^{IRAP9}$ compared to NIL-$DNR1^{HJX74}$ [9]. As a result, NO_3^- uptake capacity is reduced in NIL-$DNR1^{IRAP9}$, similar to that observed in NIL-$OsWRKY23^{IRAT261}$. With the discovery that OsWRKY23 upregulates *DNR1* expression, we tested if OsWRKY23 and DNR1 form a regulatory module governing NO_3^- uptake by comparing NO_3^- uptake rate and NR activity of HJX74 and the following NILs in the HJX74 background: NIL-$DNR1^{IRAP9}$, NIL-$OsWRKY23^{IRAT261}$, and NIL-$OsWRKY23^{IRAT261}DNR1^{IRAP9}$ (Supplementary Fig. 10a). Remarkably, NIL-$OsWRKY23^{IRAT261}DNR1^{IRAP9}$, carrying both *japonica OsWRKY23* and *DNR1* alleles, displayed significantly reduced NO_3^- uptake rate and NR activity compared to HJX74 and NILs carrying either *japonica OsWRKY23* or *DNR1* allele alone, indicating an additive effect of the *japonica OsWRKY23* and *DNR1* alleles on NO_3^- metabolism (Supplementary Fig. 10b, c). Notably, compared to NIL-$DNR1^{IRAP9}$ or NIL-$OsWRKY23^{IRAT261}$, NIL-$OsWRKY23^{IRAT261}DNR1^{IRAP9}$ plants also exhibited a decreased stature, increased tiller number, reduced grain number, and consequent grain yield, likely due to further decreased IAA content (Supplementary Fig. 10d–h).

https://doi.org/10.1038/s41467-025-56752-7

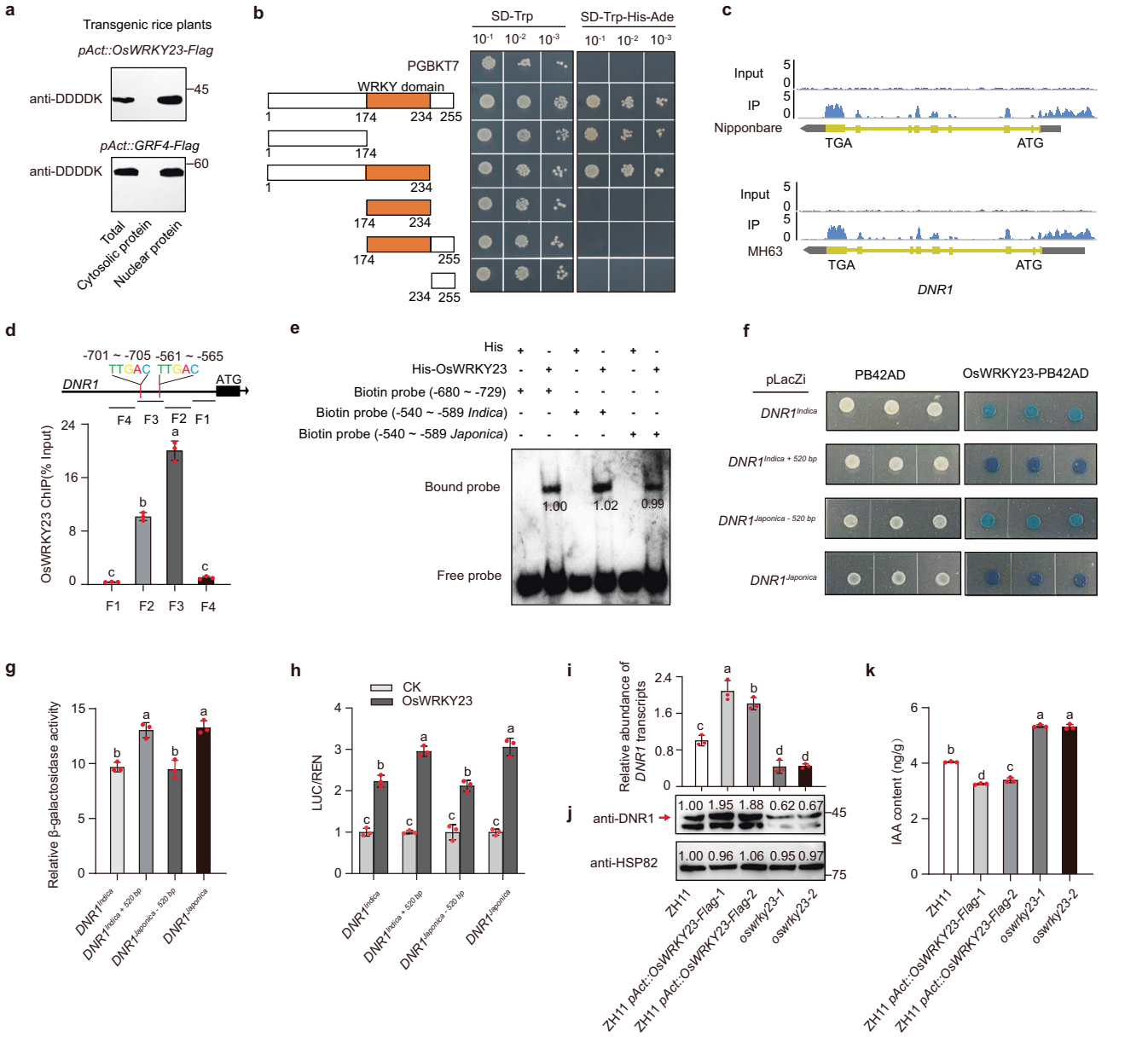

Fig. 3 | OsWRKY23 promotes *DNR1* expression. a Cellular and nuclear protein extracts were prepared by cytoplasmic and nuclear fractionation, and the presence of the OsWRKY23-Flag fusion protein was determined by immunoblotting. GRF4-Flag served as a positive control. Data are representative of three independent experiments, with similar results. **b** OsWRKY23 showed transactivation activity in yeast. Full-length, N-terminal deletion, and C-terminal deletion cDNAs of *OsWRKY23* were cloned into pGBKT7 and fused with the GAL4 DNA-binding domain. Numbers indicate the positions of the amino acid of OsWRKY23. **c** The peaks corresponding to the *DNR1* gene from ChIP-seq using the *Japonica* Nipponbare genome and *Indica* Minghui 63 (MH63) genome, respectively. **d** OsWRKY23-Flag mediated ChIP-qPCR enrichment (relative to input) of TTGAC/AACTG core sequence-containing promoter fragments from *DNR1*. **e** His-OsWRKY23 binds to TTGAC/AACTG motif-containing DNA fragments from *DNR1*. Data are representative of three independent experiments, with similar results. **f**, **g** Yeast one-hybrid assays. DNA fragments upstream of the *DNR1* of HJX74 (~2.5 kb, -2.5 kb + 520 bp) and IRAP9 (~3 kb, -3 kb - 520 bp) were used to construct the lacZi expression vectors. **h** Transactivation assay. The luciferase (LUC)/renilla (REN) activity induced by the respective *DNR1* promoters of HJX74 (~2.5 kb, -2.5 kb + 520 bp) and IRAP9 (~3 kb, -3 kb - 520 bp). The activity of the empty effector construct was set to 1. **i**, **j** Root *DNR1* transcript abundance (**i**) and root DNR1 protein abundance (**j**). Transcript abundance was measured relative to ZH11 (set to 1). HSP82 serves as loading control. The red arrow indicates the DNR1 bands. **k** Root IAA content. **d**, **g**, **h**, **i** and **k** Different letters denote significant differences ($P < 0.05$) from a two-side Duncan's multiple range test. Data are mean ± s.e.m. ($n = 3$ biological replicates). Source data are provided as a Source Data file.

Subsequently, we performed epistasis analysis to confirm that *DNR1* acts downstream of OsWRKY23, by comparing NO_3^- uptake capacity and NR activity of *oswrky23*, *dnr1*, and the *oswrky23 dnr1* double mutant. Notably, NO_3^- uptake and NR activities were significantly higher in the *oswrky23 dnr1* mutant compared to *oswrky23*, and similar to *dnr1*, due to the similarly high auxin levels in *oswrky23 dnr1* and *dnr1* relative to *oswrky23* (Fig. 4a–d). Consistently, the *oswrky23 dnr1* mutant exhibited agriculturally favorable phenotypes similar to *dnr1*, including slightly elevated plant height, reduced tillering, increased grain number and yield (Fig. 4e–h). These findings collectively indicate that OsWRKY23 acts upstream of *DNR1*, regulating auxin accumulation, N metabolism, and ultimately grain yield.

DNR1 inhibits auxin accumulation, and thereby represses the expression of genes related to NO_3^- metabolism through AUXIN

https://doi.org/10.1038/s41467-025-56752-7

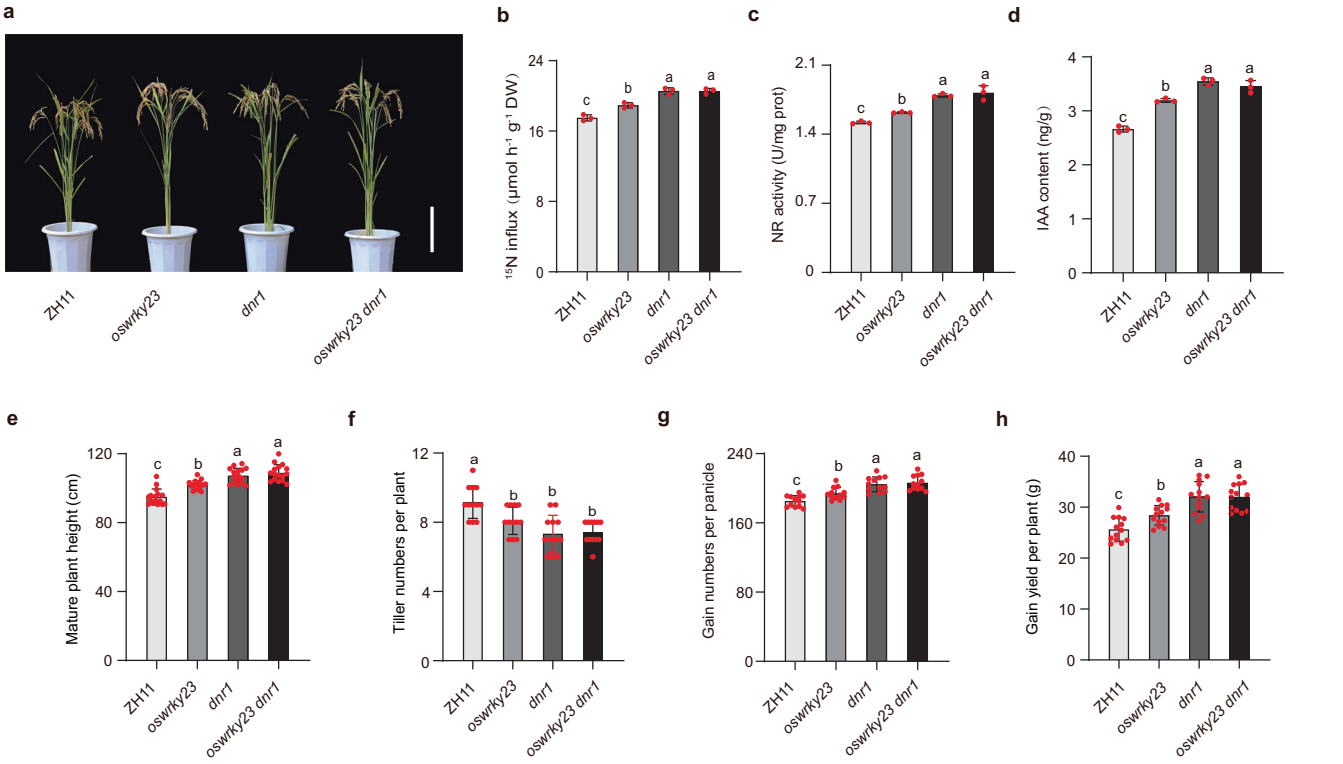

Fig. 4 | *OsWRKY23* acts upstream of *DNR1* to regulate N metabolism and grain yield. a Morphology of mature ZH11, *oswrky23*, *dnr1* and *oswrky23 dnr1* plants. Scale bar, 20 cm. **b**–**g** $^{15}NO_3^-$ uptake rate (**b**), NR activity (**c**), IAA content (**d**), plant height (**e**), the number of tillers per plant (**f**), the number of grains (**g**), and grain yield per plant (**h**) of ZH11, *oswrky23*, *dnr1* and *oswrky23 dnr1* plants. Different letters denote significant differences ($P < 0.05$) from a two-side Duncan's multiple range test. **b**–**d** Data are mean ± s.e.m. ($n = 3$ biological replicates). **e** Data are mean ± s.e.m. ($n = 16$ biological replicates). **f**–**h** Data are mean ± s.e.m. ($n = 12$ biological replicates). Source data are provided as a Source Data file.

RESPONSE FACTORS (ARFs), particularly OsARF6 and OsARF17[9]. We found that the transcript levels of both OsARF6 and OsARF17, as well as genes involved in NO_3^- uptake (e.g. *OsNRT1.1B*, *OsNRT2.3a* and *OsNPF2.4*) and NO_3^- assimilation (e.g. *OsNIA2*), were higher in the *oswrky23* mutant and lower in the *pAct::OsWRKY23-Flag* overexpression lines (Fig. 5a–f). Next, we generated *OsARF6* or *OsARF17* overexpression plants in the ZH11/*pAct::OsWRKY23-Flag* background (Fig. 5g; Supplementary Fig. 11), which showed elevated expression levels of *OsNRT1.1B*, *OsNRT2.3a*, *OsNPF2.4* and *OsNIA2* (Fig. 5h, i; Supplementary Fig. 12), thus effectively mitigating the NO_3^- uptake and NR activity deficiencies induced by *OsWRKY23* overexpression (Fig. 5j, k). However, the partial recovery in NO_3^- uptake rate and NR activity upon overexpressing *OsARF6* or *OsARF17* suggested potential functional redundancy among OsARFs in regulating NO_3^- uptake and assimilation. Integrating these findings, it became evident that OsWRKY23-mediated auxin homeostasis enhances N metabolism and rice yield through OsARFs.

Low *OsWRKY23* levels confer advantage in NUE and grain yield under low N conditions

As described above, we discovered that the *OsWRKY23* alleles of the 12 *indica* and 12 *japonica* varieties from our collection differ regarding the presence or absence of a 393-bp promoter segment, with *indica* varieties lacking it and *japonica* varieties possessing it. Further phylogenetic analysis using the public available genotype data of 3024 rice accessions[13] showed that *indica* and *japonica* *OsWRKY23* alleles belonged to two separate clades (Fig. 6a). Moreover, we found that the 393-bp segment was also associated with 14 SNPs in the promoter region that distinguished the *OsWRKY23* allele between the two subspecies. To broaden the scope of our findings, we performed a haplotype analysis of the *OsWRKY23* promoter across the 3024 rice accessions, unveiling four distinct haplotypes (Hap. I-IV). Remarkably, haplotype I and haplotype II collectively dominated the population, accounting for 82.8% of the rice accessions. Haplotype I was prevalent in *indica* varieties (97.7%) and did not contain the aforementioned 393-bp fragment in the promoter region. Conversely, haplotype II harbored this 393-bp promoter fragment and was found mainly in *japonica* varieties (84.3%) (Fig. 6b). This distinct separation of *OsWRKY23* haplotypes prompted us to investigate whether the allele distribution of *OsWRKY23* in different rice subgroups correlates with their environmental condition, particularly soil N content. To this end, we gathered data on soil total N content in rice planting areas from 42 countries or regions. Upon projecting all varieties back to their original locations, we uncovered a robust association between haplotype and soil N content. Specifically, haplotype I varieties predominated regions with relatively low soil total N whereas haplotype II varieties were extensively cultivated in N-rich areas (Fig. 6c). This suggests that the two variants of *OsWRKY23* with different expression levels might have played a pivotal role in the geographical adaptation of rice varieties to soil with different N content.

To further decipher the evolutionary trajectory of the *OsWRKY23* gene in different rice varieties, we used the 393-bp segment as a marker and analyzed the promoter sequence of *OsWRKY23* in 185 wild rice varieties, including those from OR-I (ancestors of Aus and *indica* varieties), OR-J (ancestors of tropical and temperate *japonica* varieties), and OR-W (other wild rice varieties) clades. Interestingly, all OR-J varieties harbored the 393-bp fragment in their *OsWRKY23* promoters, whereas in contrast to the prevalent absence of this fragment in modern *indica* rice, only 6 varieties (11.1%) within the OR-I clade had *OsWRKY23* promoters without this fragment. These results suggest a pronounced selection pressure favoring either the loss (in *indica*) or

https://doi.org/10.1038/s41467-025-56752-7

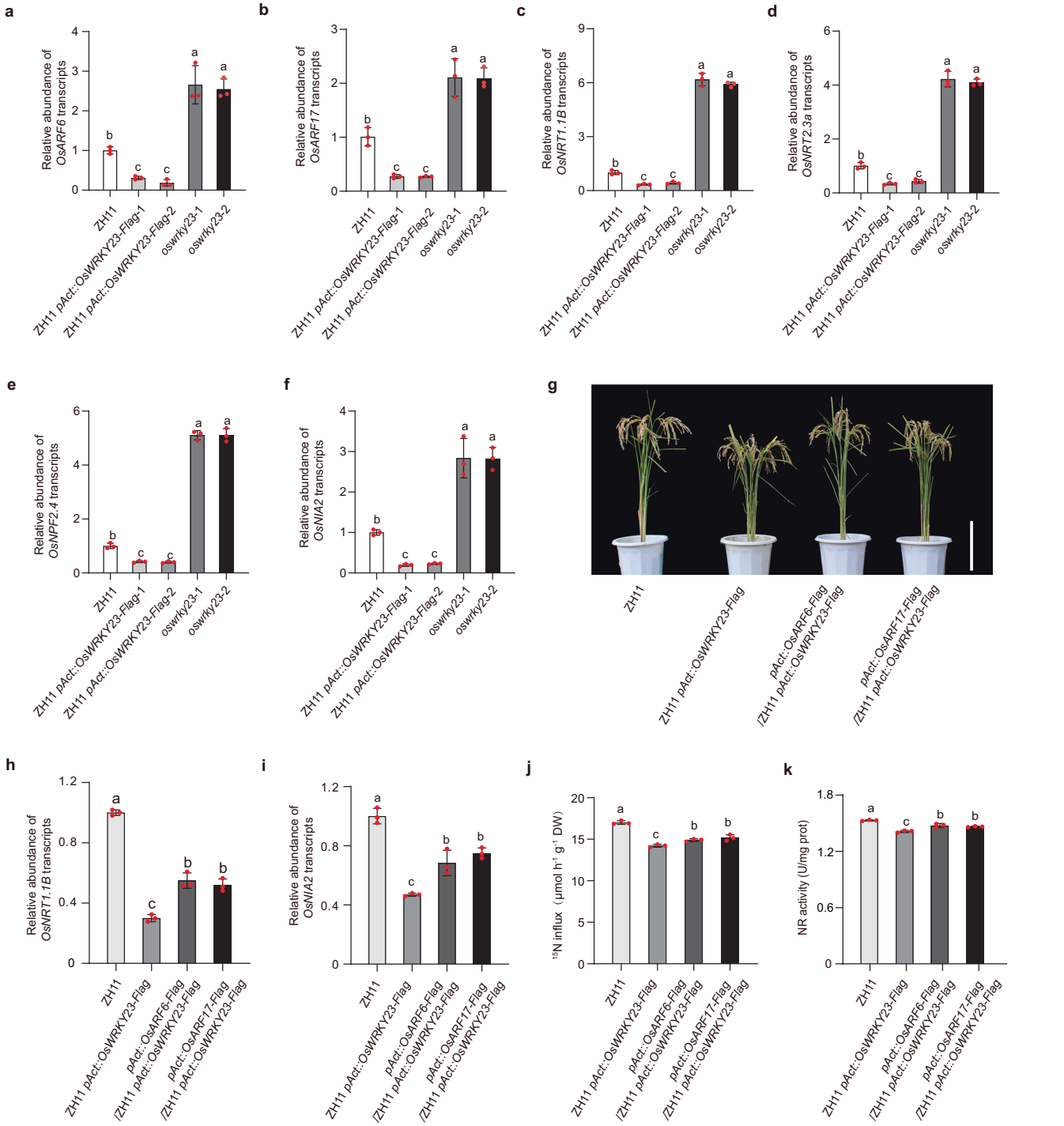

Fig. 5 | The OsWRKY23-DNR1 module regulates N metabolism-related genes and thereby N metabolism through OsARFs. a–**f** mRNA abundances of *OsARF6* (**a**), *OsARF17* (**b**), *OsNRT1.1B* (**c**), *OsNRT2.3a* (**d**), *OsNPF2.4* (**e**), and *OsNIA2* (**f**) relative to ZH11 (set to 1). Data are mean ± s.e.m. ($n = 3$ biological replicates). **g** Morphology of mature ZH11, ZH11/*pAct::OsWRKY23-Flag*, and *OsARF6* and *OsARF17* overexpression lines in the ZH11/*pAct::OsWRKY23-Flag* background. Scale bar, 20 cm. **h**, **i** mRNA abundances of *OsNRT1.1B* (**h**) and *OsNIA2* (**i**) relative to ZH11 (set to 1). **j** $^{15}NO_3^-$ uptake rate. **k** NR activity. **a**–**f**, **h**–**k** Different letters denote significant differences ($P < 0.05$) from a two-side Duncan's multiple range test. Data are mean ± s.e.m. ($n = 3$ biological replicates). Source data are provided as a Source Data file.

retention (in *japonica*) of the 393-bp fragment in the *OsWRKY23* promoter (Fig. 6d).

After establishing the OsWRKY23-DNR1-auxin regulatory module for N metabolism and grain yield, we compared the distribution pattern of *OsWRKY23* and *DNR1* haplotypes, which closely aligned with each other (Supplementary Table 1). Moreover, the distribution of the *indica* haplotype I of *OsWRKY23* showed a positive correlation with the distribution of the *indica* haplotype I of *DNR1*, while the distribution of the *japonica* haplotype II of both genes also exhibited a positive correlation across the 78 countries where the rice accessions used for haplotype analysis for *OsWRKY23* and *DNR1* were located (Fig. 6e, f). Conversely, the distribution of the *indica* haplotype I of *OsWRKY23* was negatively correlated with the *japonica* haplotype II of *DNR1* (Fig. 6g, h). These findings further underscored the coordinated

https://doi.org/10.1038/s41467-025-56752-7

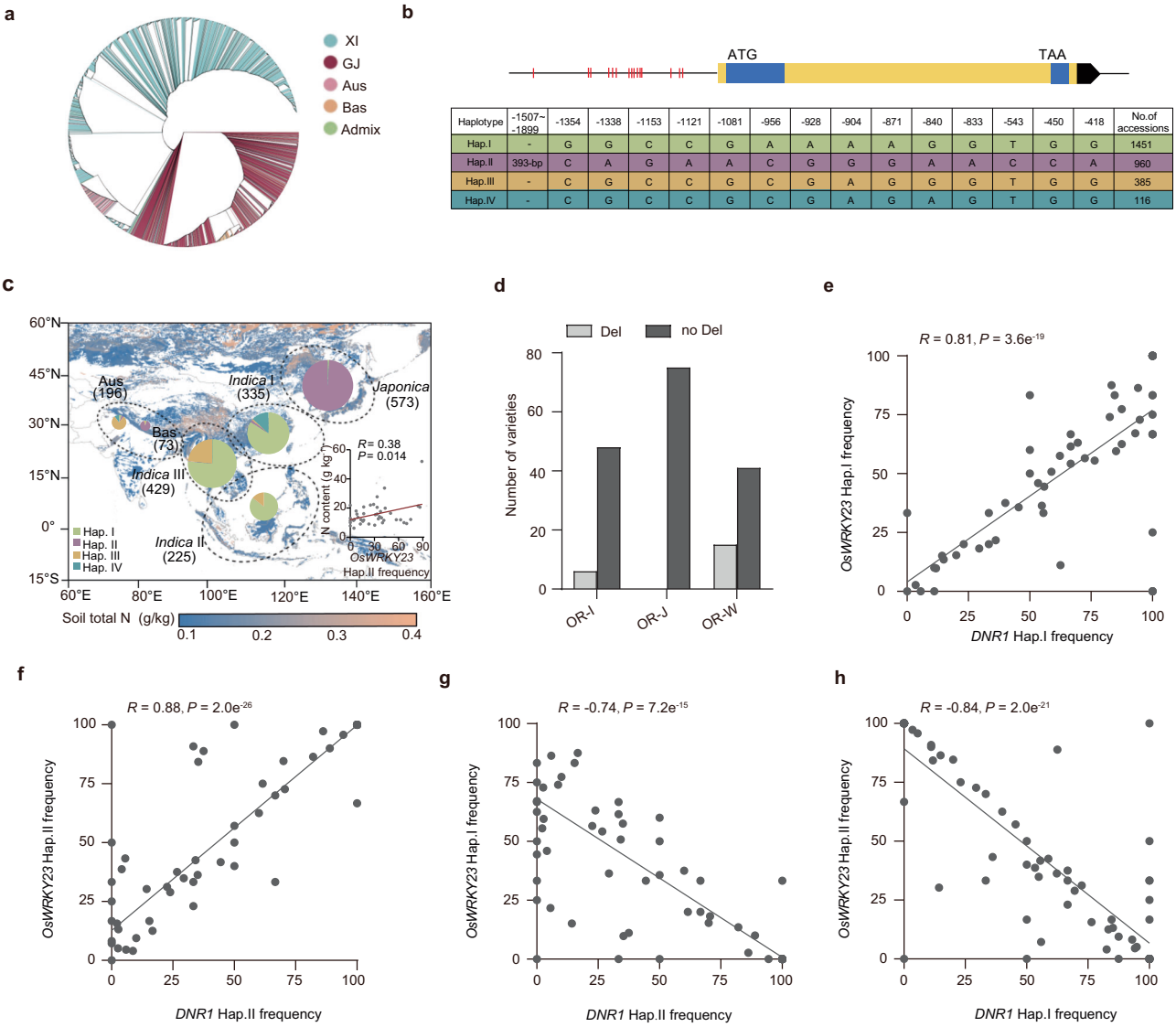

Haplotype	-1507~-1899	-1354	-1338	-1153	-1121	-1081	-956	-928	-904	-871	-840	-833	-543	-450	-418	No.of accessions
Hap.I	-	G	G	C	C	G	A	A	A	A	G	G	T	G	G	1451
Hap.II	393-bp	C	A	G	A	A	C	G	G	G	A	A	C	C	A	960
Hap.III	-	C	G	C	C	G	C	G	A	G	G	G	T	G	G	385
Hap.IV	-	C	G	C	C	G	C	G	A	G	A	G	T	G	G	116

Fig. 6 | Phylogenetic and functional analyses of *OsWRKY23* haplotypes. **a** Phylogenetic tree of *OsWRKY23* from 3024 rice accessions. Blue: *indica*; red: *japonica*; pink: Aus; orange: Bas; green: admix. **b** DNA polymorphisms in the promoter and gDNA of *OsWRKY23*. "-" indicates deletion. **c** OsWRKY23-Hap II frequency is highly correlated with soil N content in 42 countries. **d** The presence or absence of the 393-bp INDEL in the three clades of wild rice varieties. **e**–**h** Pearson correlation analysis of different haplotypes of *OsWRKY23* and *DNR1* in 78 countries. Source data are provided as a Source Data file.

regulatory role of these two genes in modulating the variation in NO_3^- uptake observed between *indica* and *japonica* rice varieties.

Finally, we explored the potential of *OsWRKY23* as a target for enhancing the agronomic traits of *japonica* rice varieties. To this end, we examined the phenotypes of ZH11, *oswrky23*, and the *oswrky23 dnr1* double mutant. Compared to the WT control, *oswrky23* plants exhibited moderately increased height and reduced tillering under both high and low N conditions. Notably, *oswrky23* plants showed similar number of primary branches but an increased number of secondary branches per panicle, which led to a significant enhancement in grain yield. Importantly, under both high and low N conditions, the *oswrky23 dnr1* double mutant exhibited enhanced agronomic traits compared to *oswrky23*. This highlights the potential for yield improvement through optimizing the OsWRKY23-DNR1 module (Fig. 7).

Discussion

Asian cultivated rice comprises two major subspecies: *indica* and *japonica*, each characterized by distinct developmental and physiological traits[14,15]. *Japonica* varieties, representing about 40% of rice cultivation in China, Japan, and South Korea[16], excel in both food quality and yield stability, particularly thriving in cooler climates[14,15]. However, *japonica* varieties exhibit lower efficiency in NO_3^- uptake and assimilation compared to *indica* varieties, resulting in reduced NUE[5]. To address this weakness of *japonica* varieties, it is crucial to identify alleles conferring efficient NO_3^- utilization in *indica* varieties and integrate them into *japonica* varieties. In this study, we identified *OsWRKY23*, a negative regulator of NO_3^- uptake, from a SSSL carrying a single chromosome segment from a *japonica* variety (IRAT261) into the *indica* (HJX74) genetic background that exhibited a reduced NO_3^- uptake rate compared to its *indica* parent.

OsWRKY23 belongs to the WRKY superfamily of transcription factors that are primarily found in higher plants, with *Arabidopsis* hosting 74 members and rice potentially accommodating up to 116 in *Indica* rice and 137 in *Japonica* rice[17]. Functionally, WRKY proteins play crucial roles in regulating a variety of biotic and abiotic stress responses in plants, ranging from pathogen attacks to environmental stresses such as salinity, drought and cold[17–29], as well as developmental processes such as leaf senescence, trichome

https://doi.org/10.1038/s41467-025-56752-7

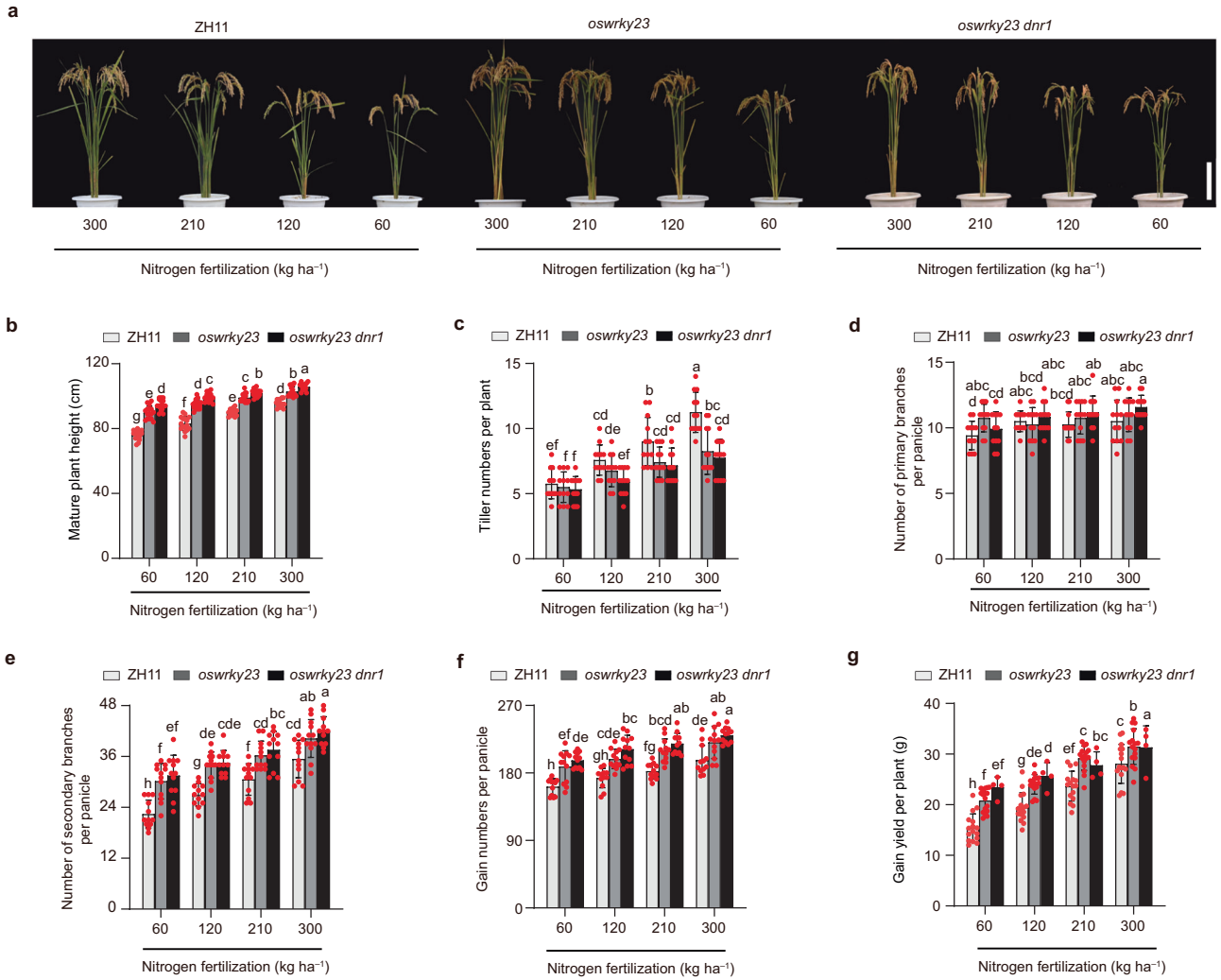

Fig. 7 | *oswrky23* and *oswrky23 dnr1* have higher NUE and grain yield. **a** Morphology of mature ZH11, *oswrky23* and *oswrky23 dnr1* plants, grown at different N supply. Scale bar, 20 cm. **b**–**g** Plant height (**b**), the number of tillers per plant (**c**), the number of primary branches per plant (**d**), the number of secondary branches per plant (**e**), the number of grains per panicle (**f**), and grain yield per plant (**g**) of ZH11, *oswrky23* and *oswrky23 dnr1* plants. **b**–**g** Different letters denote significant differences ($P < 0.05$) from a two-side Duncan's multiple range test. **b** Data are mean ± s.e.m. ($n = 16$ biological replicates). **c**–**g** Data are mean ± s.e.m. ($n = 12$ biological replicates). Source data are provided as a Source Data file.

development, embryogenesis, carbohydrate anabolism and secondary metabolism[30,31]. Several previous studies have alluded to a regulatory role played by WRKY family members on N pathway[32–38]. First, WRKY proteins have been shown to participate in the process of leaf senescence, during which more than 70% of leaf N is estimated to be exported from senescing leaves throughout the seed filling stage in most annual crops as a mean of N remobilization. For example, *AtWRKY70*, *AtWRKY53*, *AtWRKY75*, and *HvWRKY12* exhibit high expression levels in senescing leaves, therefore playing a regulatory role in leaf sentence[32–34]. Additionally, aberrant methylation of W-box sequences might disrupt signal transduction networks involving AtWRKY53, AtWRKY18, and AtWRKY25 during senescence[35]. Second, AtWRKY1 is responsible for integrating signals related to cellular N and light-energy resources to regulate changes in plant metabolism[36]. Third, glutamine, the downstream assimilation product of N metabolism, induces the expression of *WRKY8*, *WRKY25*, *WRKY28*, *WRKY29*, *WRKY31*, *WRKY42*, and *WRKY48*, as well as JA-responsive gens *WRKY50* and *WRKY51*, to regulate *Arabidopsis* stress responses[37]. Finally, WRKY-binding sites were found to be enriched in the promoters of genes induced by nitric oxide (NO), a key signaling molecule involved in various physiological processes that is synthesized from nitrite and L-arginine[38]. However, to our best knowledge, the direct regulation of NO_3^- uptake by a WRKY family protein has not been reported before, highlighting the unique role of OsWRKY23 in rice.

OsWRKY23 acts as a transcriptional activator that directly binds to the promoter region of *DNR1* to induce its expression. As a negative regulator of auxin accumulation, increased DNR1 level reduces auxin level, which results in a diminished capacity of OsARFs to stimulate downstream genes related to N metabolism. Therefore, the OsWRKY23-DNR1 module negatively impacts rice NUE (Supplementary Fig. 13). Given the regulatory role played by DNR1 on aboveground phenotypes[9] that are also influenced by OsWRKY23, it is possible that the mRNA or protein of OsWRKY23 translocate from root to shoot to modulate the level of DNR1 in the shoot. However, the facts that the expression patterns of *OsWRKY23* and *DNR1* largely overlapped, and both the transcript and protein levels of *OsWRKY23* and *DNR1* were positively regulated by external N in the shoot (similar to what occurs in the root, Supplementary Fig. 9)[10], do not lend support to this hypothesis. Nevertheless, further evidence is needed to confirm this. Additionally, we also explored the possibility of OsWRKY23 directly targeting genes involved in auxin signaling, NRTs, and NIAs for

transcriptional regulation. We discovered the presence of W-box motifs in the promoter regions of some of these genes, suggesting that OsWRKY23 has the potential to regulate their transcription. For instance, in the ~3 kb promoter sequence of *OsNRT1.1B*, we identified three W-boxes located at positions -2201 ~ -2205, -2104 ~ -2108, and -552 ~ -556, and demonstrated that OsWRKY23 could bind to these three core sequences and activate its expression. However, such regulation is inconsistent with the observed decrease in *OsNRT1.1B* expression in *OsWRKY23* overexpression lines, indicating that any promotion of *OsNRT1.1B* expression by OsWRKY23 is likely outweighed by its activation of DNR1-mediated inhibition on *OsNRT1.1B* expression, thus leading to the inhibition of NO_3^- uptake (Supplementary Fig. 14).

Interestingly, we discovered evident disparities in the promoter sequence of *OsWRKY23* between *indica* and *japonica* rice varieties, especially regarding the presence or absence of a 393-bp fragment. *Indica* varieties generally lack this 393-bp region and exhibit a lower *OsWRKY23* expression level, which contributes to the higher NUE observed compared to *japonica* varieties (Supplementary Fig. 13). These results elude to the potential of manipulating *OsWRKY23* expression level, especially in *japonica* varieties, for enhanced NUE.

To this end, we generated null *oswrky23* mutant lines and *oswrky23 dnr1* double mutant lines in the *japonica* ZH11 background. Notably, when compared to WT plants, both NUE and grain yield exhibited significant improvements in both *oswrky23* and *oswrky23 dnr1* due to increased auxin accumulation, with the above-ground architecture moderately affected. Hence, we propose that the OsWRKY23-DNR1-auxin cascade presents a promising avenue for improving crop NUE, thereby promoting sustainable agriculture in the future.

Methods

Plant materials and field growth conditions

The *indica* HJX74 and *japonica* IRAT261 rice germplasms were used in this study for constructing the SSSLs and mapping populations. This included BC_1F_2 and BC_2F_2 populations derived from a cross with SSSL-W56, containing a substituted segment from IRAT261 in the genetic background of HJX74, which served as the recipient parent[11]. Paddy-grown rice plants were grown under standardized conditions at two experimental stations: one situated in Lingshui, Hainan Province, and the other in Hefei, Anhui Province.

Hydroponic culture of plants

Seeds were sterilized using a 20% NaClO solution for 30 minutes, and uniform seedlings were selected for further analyses. Seven-day-old seedlings were then transferred and grown in 40 L of nutrient solution (0.625 mM $(NH_4)_2SO_4$, 1.25 mM KNO_3, 0.3 mM $NaH_2PO_4{\cdot}2H_2O$, 1 mM $CaCl_2$, 1 mM $MgSO_4{\cdot}7H_2O$, 20 μM EDTA-Fe, 0.5 mM Na_2SiO_3, 9 μM $MnCl_2$, 20 μM H_3BO_3, 0.77 μM $ZnSO_4$, 0.32 μM $CuSO_4$, 0.39 μM $(NH_4)_6Mo_7O_{24}$, pH 5.5) in PVC pots for four weeks. To vary N concentrations as needed, 0.625 mM $(NH_4)_2SO_4$ and 1.25 mM KNO_3 (1 N) was replaced with 0.375 mM $(NH_4)_2SO_4$ and 0.75 mM KNO_3 (0.6 N), 0.1875 mM $(NH_4)_2SO_4$ and 0.375 mM KNO_3 (0.3 N), or 0.09375 mM $(NH_4)_2SO_4$ and 0.1875 mM KNO_3 (0.15 N). Nutrient solutions were replenished twice weekly, and pH levels were adjusted to 5.5 daily using 5 M NaOH. The growth conditions maintained a temperature of 30 °C during the 14 h of light and 22 °C during the 10 h of darkness, with a photon density of 400 μmol/s/m² and a relative humidity of 60%.

Fine mapping of *OsWRKY23*

Fine mapping of *OsWRKY23* utilized BC_1F_2 and BC_2F_2 plants derived from backcrossing a selected SSSL-W56 with HJX74. Detailed primer sequences for map-based cloning can be found in Supplementary Table 2.

Transgene constructs

The full-length *OsWRKY23*, *OsARF6*, and *OsARF17* cDNA were amplified from ZH11 and subsequently inserted into the *pAct::Flag-nos* vector to generate the *pAct::OsWRKY23-Flag*, *pAct::OsARF6-Flag* and *pAct::OsARF17-Flag* constructs[10]. gRNA constructs required for generating the CRISPR/Cas9-induced loss-of-function mutations in *OsWRKY23* within the ZH11 genetic background, as well as in both *OsWRKY23* and *DNR1* within the ZH11 genetic background, were prepared following established protocols[39]. Transgenic rice plants were generated via *Agrobacterium* (AGL1)-mediated transformation[40]. Details of the primer sequences used are provided in Supplementary Table 3.

Subcellular localization

To determine the subcellular localization of OsWRKY23, the full-length cDNA of OsWRKY23 was fused in-frame to the green fluorescent protein (GFP) and driven by its ~3 kb native promoter to generate the *pOsWRKY23-OsWRKY23-GFP-nos* vector. The nucleus-localized gene *OsWRKY29* was constructed in the *p35S::mCherry-nos* vector (35S promoter from the Cauliflower Mosaic Virus (CaMV)) to indicate nuclear localization signals. The localization of GFP was visualized 24 h using a confocal microscope (Zeiss LSM710). Detailed primer sequences can be found in Supplementary Table 3.

Preparation of nuclear and cellular protein extracts

An extraction buffer containing Ficoll (25 mg/mL), Dextran T 40 (50 mg/mL), Sucrose (137 mg/mL), 25 mM Tris-HCl (pH 7.4), 10 mM $MgCl_2$, 0.5 mM DTT, and a protein inhibitor cocktail (Roche Life-Science) was used to separate cytoplasmic and nuclear proteins. OsWRKY23-Flag and GRF4-Flag proteins from *OsWRKY23* and *GRF4* overexpression lines[41], respectively, were detected by immunoblotting using anti-DDDDK (MBL, 185-7, Lot.009, diluted 1:10000). Immunoblotting results were visualized using the Tanon-5200 Chemiluminescent Imaging System (Tanon Science and Technology).

Transcription activation assay in yeast

The full-length and domain-specific fragments of OsWRKY23 cDNA were separately inserted into the *PGBKT7* vector (Takara). The resulting constructs were transformed into yeast strains (AH109) and cultured on selective media: single dropout medium (SD-Trp) and triple dropout medium (SD-Trp-His-Ade). Detailed primer sequences are provided in Supplementary Table 3.

Quantitative real time PCR analysis

Total RNAs were extracted from various plant tissues using the TRIzol reagent (Tsingke, TSP401), and full-length cDNAs were synthesized using a cDNA synthesis kit (Accurate Biology, AG11728). RT-qPCR was conducted following the manufacturer's protocol (Accurate Biology, AG11718). Each RT-qPCR assay included a minimum of three biological replicates. The rice *ACTIN1* gene (*OsActin1*, LOC_Os03g50885) served as the internal reference. RT-qPCR primer sequences are detailed in Supplementary Table 4.

ChIP-seq and ChIP-qPCR assays

For ChIP assays, approximately 2 g of 14-day-old seedlings from transgenic *pActin::Flag-OsWRKY23* rice plants were fixed with 1% (v/v) formaldehyde. After isolating and lysing nuclei, chromatin complexes were extracted and sonicated to yield fragments averaging ~500 bp in size. Immunoprecipitation was performed overnight at 4 °C using anti-Flag antibodies (Sigma, F1804). The precipitated DNA was eluted and stored in water at -80 °C. Sequencing libraries were prepared according to the manufacturer's protocol and sequenced on the BGISEQ-500 platform. Sequence reads were aligned to the reference genomes of Nipponbare and Minghui 63 (MH63), respectively. Additionally, precipitated DNA samples were used as templates for RT-qPCR, with primer sequences provided in Supplementary Table 4.

EMSA assays

Full-length *OsWRKY23* cDNA was inserted into the pCold-TF vector (Takara), which was subsequently transferred to *E. coli* BL21 (DE3; Sangon Biotech, B528414-0100) under the induction condition of 18 °C at 150 rpm for 12 h with 0.3 mM IPTG to facilitate the expression of the His-OsWRKY23 recombinant protein. His-OsWRKY23 was then purified using Ni-NTA agarose beads (QIAGEN, 30210) following the manufacturer's protocol. DNA probes were amplified and labeled with biotin using a biotin labeling kit (Sangon Biotech). DNA gel shift assays were conducted using the LightShift Chemiluminescent EMSA kit (Thermo Fisher Scientific, 20148). Detailed primer sequences can be found in Supplementary Table 5.

Yeast one-hybrid assays

The OsWRKY23 cDNA was inserted into the *pB42AD* vector (Takara). Promoter fragments of ~3 kb and 2.5 kb corresponding to *DNR1* were amplified from IRAP9 and HJX74, respectively. The ~2.5 kb fragment from IRAP9 had the 520-bp region removed, while the ~3 kb fragment from HJX74 had this region inserted. All fragments were then cloned into the pLacZi vector to drive the *lacZ* reporter gene expression[42,43]. The constructs were subsequently introduced into the yeast strain EGY48. Monoclonal colonies were selected from SD-Trp/Ura plates, and then cultured in SD-Ura liquid medium for 48 h. The yeast culture was collected in 2 mL tubes, and the experimental procedures were performed following the manufacturer's instructions, with β-galactosidase activity assessed at 420 nm using a spectrophotometer[44]. Detailed PCR primer sequences can be found in Supplementary Table 6.

Transient expression assays in rice protoplasts

The ~3 kb and ~2.5 kb promoter fragments of *DNR1* were amplified from IRAP9 and HJX74, respectively. The ~2.5 kb fragment from IRAP9 had the 520-bp region removed, while the ~3 kb fragment from HJX74 had this region inserted. Both fragments were cloned into the pUC19 vector. These constructs contained the firefly luciferase (LUC) reporter gene driven by the 35S minimal TATA box and 5× GAL4 binding elements[45–47]. Full-length cDNA of *OsWRKY23* was amplified and fused with the GAL4 binding domain (GAL4BD) sequence to generate the effector plasmid *pRTBD-OsWRKY23*. Transient transactivation assays were performed using rice protoplasts. Briefly, the plasmid was added to a 2 mL tube, followed by 100 µL of rice protoplasts and 110 µL of 40% PEG4000. The mixture was gently shaken and incubated in the dark for 15 minutes. The reaction was terminated by adding 440 µL of W5 solution, followed by centrifugation to remove the supernatant. The protoplasts were then washed once with W5, resuspended in 1 mL of W5, and incubated at 28°C for 16 h. LUC activity assays were conducted using the Dual-LUC Reporter Assay System (Promega, Madison, WI, USA; E1960) and the GloMax™ 20-20 Luminometer, with the Renilla (REN) LUC gene serving as the internal control[48]. PCR primer sequences are provided in Supplementary Table 7.

Western blotting

Total protein was extracted from root tips using extraction buffer containing 50 mM Tris-HCl (pH 7.5), 150 mM NaCl, 0.1% NP-40 detergent, 10% Glycerol, 1 mM DTT and protease inhibitor cocktail (Roche LifeScience). The proteins were separated by SDS-PAGE electrophoresis. OsWRKY23 and DNR1 proteins were detected by immunoblotting using anti-OsWRKY23 antibodies (customized in the Animal Experiment Center, Institute of Genetics and Developmental Biology, Chinese Academy of Sciences, diluted 1:2000), anti-DNR1 antibodies (ABclonal, diluted 1:5000), and anti-DDDDK-tag antibodies (MBL, 185-7, Lot.009, diluted 1:10000), respectively. Immunoblotting results were visualized using the Tanon-5200 Chemiluminescent Imaging System (Tanon Science and Technology).

^{15}N uptake analysis

After growth in hydroponic condition for 21 days, rice root low-affinity $^{15}NO_3^-$ influx measurements were conducted as follows. Specifically, 21-day-old rice plants were initially transferred to 0.1 mM $CaSO_4$ for 1 min, followed by a complete nutrient solution containing 2.5 mM $K^{15}NO_3$ (Aldrich, 335134, 98% atom excess ^{15}N) as the N source, replacing 0.625 mM $(NH_4)_2SO_4$ and 1.25 mM KNO_3, for 5 min. After this, the plants were incubated in 0.1 mM $CaSO_4$ for 1 min before collecting the roots, which were dried at 80 °C for 72 h. Root dry weight was recorded, and the ^{15}N content was measured using the Isoprime 100 (Elementar, Germany). The influx of $^{15}NO_3^-$ was calculated from δ (‰ min^{-1}), N content (N%), and entire root dry weight (DW) as follow:

$$\delta^{15}N\,(‰\cdot \mathrm{min}^{-1}) = \frac{R_{SAMPLE} - R_{STD}}{R_{STD}} \cdot 10^3 \quad (1)$$

R_{SAMPLE} is the $^{15}N/^{14}N$ ratio of the sample and R_{STD} is the $^{15}N/^{14}N$ ratio of atmospheric N_2.

$$^{15}N\,\mathrm{influx}\,(\mu\mathrm{mol}\cdot \mathrm{h}^{-1}\cdot \mathrm{g}^{-1}\cdot \mathrm{DW}) = \frac{24000\cdot \mathrm{DW}\cdot N\%R_{STD}\cdot(\delta^{15}N + 200)}{560 + 3\cdot R_{STD}\cdot(\delta^{15}N + 200)} \quad (2)$$

N% is the N content and DW is the dry weight of whole root.

Measurement of NR activity

Approximately 1 g of fresh plant material from individual rice plant was used to assess NR activity, following the instructions provided in the Nitrate Reductase Kit (Solarbio LIFE SCIENCES, BC0080).

Determination of IAA content

Approximately 50 mg of root tips were ground into a fine powder in liquid N and extracted with an acetonitrile solution[9]. The concentration of IAA was subsequently determined using an ESI-HPLC-MS/MS system and a standard curve provided by Wuhan Triploid Biotech.

Root system analysis

Roots from rice plants were excised and spread out in water within a transparent dish. The root system was then scanned using a ScanMaker i800plus (Zhejiang TOP Cloud-agri Technology Company) with a resolution set to 300 dpi and a zoom ratio of 100%. The scanned image was imported into the RhizoPheno root analysis system (Zhejiang TOP Cloud-agri Technology Company) to measure the total root length, area and number. Objects smaller than 10 pixels were automatically excluded by the software as noise or contamination.

Bioinformatic analysis of functional genes based on the 3 K RG panel

Bioinformatic analysis of functional genes based on the 3 K RG panel was performed for haplotype analyses of *OsWRKY23* and *DNR1*. INDELs and a base set of approximately 18 million SNPs from all 3024 lines were sourced and analyzed[10,12].

Analysis of the resequence data of wild rice

Resequencing data from 185 wild rice samples were obtained from a previous study[49]. Raw reads were processed using Trimmomatic for quality control, then aligned to the *japonica* reference genome (Nipponbare, Reference-IRGSP-1.0) with BWA, employing default parameters[50]. Duplicate reads were removed using Picard tools, and pairs with a mapping quality below 10 were excluded. Only paired reads with valid mapping were retained. Structural variations were identified using Lumpy with default settings[51].

Geographical distribution of rice varieties and soil nitrogen content analysis

The soil total nitrogen content for 42 rice-growing countries was obtained from a previous study[52]. For detailed information, 5-arc-minute maps of soil nitrogen content were aggregated into country-scale and vertically-lumped data using area- and depth-weighted methods to align with the spatial scale of *OsWRKY23* allele frequency. First, soil nitrogen content data were sourced from a comprehensive global soil dataset (http://globalchange.bnu.edu.cn) at a spatial resolution of 5′ × 5′. To represent the average nitrogen content within the root zone, we calculated a weighted average of soil nitrogen across four soil layers: 0–4.5 cm, 4.5–9.1 cm, 9.1–16.6 cm, 16.6–28.9 cm. Subsequently, data on rice-planting areas (km^2 for each grid cell) from recent decades were obtained from the History Database of the Global Environment (HYDE 3.2.1)[53] with a spatial resolution identical with the global soil dataset. To avoid biased estimations for countries with smaller rice-planting areas, we acquired area-weighted soil nitrogen content across all rice-planting areas within each country. Finally, Pearson's correlation analysis was performed to assess the relationship between the soil total nitrogen content of these 42 countries and the *OsWRKY23* allele frequency in the corresponding countries.

Statistical analysis

We analyzed the data from field and hydroponic experiments using two-sided Student's *t*-tests and Duncan's multiple range test. Multiple comparisons were conducted with the least significant difference test at a significance level of $P = 0.05$. All statistical analyses were performed using SPSS version 27.

Reporting summary

Further information on research design is available in the Nature Portfolio Reporting Summary linked to this article.

Data availability

The ChIP-seq data have been uploaded to NCBI Sequence Read Archive (SRA) database under accessions SRR32088468 and SRR32088469 within BioProject PRJAN1214501 [https://dataview.ncbi.nlm.nih.gov/object/PRJNA1214501]. SNPs for accessions from the 3 K Rice Genomes Project can be accessed via RiceVarMap v2.0 (http://ricevarmap.ncpgr.cn/). Resequencing data of the 185 wild rice accessions are available at NCBI. Soil nitrogen content data can be found in the Global Soil Data set (http://globalchange.bnu.edu.cn). The data for the rice-planting area of different countries are from the History Database of the Global Environment (HYDE 3.2.1) (https://doi.org/10.17026/dans-25g-gez3). Soil nitrogen content data in different countries were obtained from previous study[52]. Source data are provided with this paper.

References

1. Liu, X. et al. Enhanced nitrogen deposition over China. *Nature* **494**, 459–462 (2013).
2. Chen, X. et al. Producing more grain with lower environmental costs. *Nature* **514**, 486–489 (2014).
3. Godfray, H. C. et al. Food security: the challenge of feeding 9 billion people. *Science* **327**, 812–818 (2010).
4. Ludemann, C. I. et al. A global FAOSTAT reference database of cropland nutrient budgets and nutrient use efficiency (1961-2020): nitrogen, phosphorus and potassium. *Earth Syst. Sci. Data* **16**, 525–541 (2024).
5. Hu, B. et al. Variation in *NRT1.1B* contributes to nitrate-use divergence between rice subspecies. *Nat. Genet* **47**, 834–838 (2015).
6. Kirk, G. J. D. & Kronzucker, H. J. The potential for nitrification and nitrate uptake in the rRhizosphere of wetland plants: A modelling study. *Ann. Bot.* **96**, 639–646 (2005).
7. Gao, Z. et al. The *indica* nitrate reductase gene *OsNR2* allele enhances rice yield potential and nitrogen use efficiency. *Nat. Commun.* **10**, 5207–5210 (2019).
8. Gao, Y. et al. MYB61 is regulated by GRF4 and promotes nitrogen utilization and biomass production in rice. *Nat. Commun.* **11**, 5219–5231 (2020).
9. Zhang, S. et al. Natural allelic variation in a modulator of auxin homeostasis improves grain yield and nitrogen use efficiency in rice. *Plant Cell* **33**, 566–580 (2021).
10. Huang, Y. et al. Improving rice nitrogen-use efficiency by modulating a novel monouniquitination machinery for optimal root plasticity response to nitrogen. *Nat. Plants* **9**, 1902–1914 (2023).
11. Zhang, Y. et al. Development of a wide population of chromosome single-segment substitution lines in the genetic background of an elite cultivar of rice (Oryza sativa L. Genome 49, 476–484 (2006).
12. Ulker, B. & Somssich, L. E. WRKY transcription factors: from DNA binding towards biological function. *Curr. Opin. Plant Biol.* **7**, 491–498 (2004).
13. Wang, W. et al. Genomic variation in 3,010 diverse accessions of Asian cultivated rice. *Nature* **557**, 43–49 (2018).
14. Oka, H. I. Origin of cultivated rice (Japan Scientific Societies Press, 1983).
15. Jin, J. et al. Genetic control of rice plant architecture under domestication. *Nat. Genet* **40**, 1365–1369 (2008).
16. Purugganan, M. D. & Fuller, D. Q. The nature of selection during plant domestication. *Nature* **457**, 843–848 (2009).
17. Khoso, M. A. et al. WRKY transcription factors (TFs): Molecular switches to regulate drought, temperature, and salinity stresses in plants. *Front Plant Sci.* **13**, 1039329 (2022).
18. Asai, T. et al. MAP kinase signalling cascade in *Arabidopsis* innate immunity. *Nature* **415**, 977–983 (2002).
19. Kim, C. Y. et al. Identification of rice blast fungal elicitor-responsive genes by differential display analysis. *Mol. Plant Microbe Interact.* **13**, 470–474 (2000).
20. Seki, M. et al. Monitoring the expression profiles of 7000 *Arabidopsis* genes under drought, cold and high-salinity stresses using a full-length cDNA microarray. *Plant J.* **31**, 279–292 (2002).
21. Gulzar, F. et al. Maize WRKY transcription factor *ZmWRKY79* positively regulates drought tolerance through elevating ABA biosynthesis. *Int J. Mol. Sci.* **22**, 10080–10098 (2021).
22. Jiang, J. et al. WRKY transcription factors in plant responses to stresses. *J. Integr. Plant Biol.* **59**, 86–101 (2016).
23. Li, M. et al. Genome-wide analysis of the WRKY genes and their important roles during cold stress in white clover. *PeerJ* **11**, e15610 (2023).
24. Rai, G. K. et al. Plant salinity stress, sensing, and its mitigation through WRKY. *Front Plant Sci.* **14**, 1238507 (2023).
25. Wang, C. et al. Maize WRKY transcription factor ZmWRKY106 confers drought and heat tolerance in transgenic plants. *Int J. Mol. Sci.* **19**, 3046–3060 (2018).
26. Wang, Y. et al. A WRKY transcription factor PmWRKY57 from *Prunus mume* improves cold tolerance in *Arabidopsis thaliana*. *Mol. Biotechnol.* **65**, 1359–1368 (2023).
27. Zhang, M. et al. The OsWRKY63-OsWRKY76-OsDREB1B module regulates chilling tolerance in rice. *Plant J.* **112**, 383–398 (2022).
28. Zhang, J. et al. Drought-responsive WRKY transcription factor genes *IgWRKY50* and *IgWRKY32* from Iris germanica enhance drought resistance in transgenic *Arabidopsis*. *Front Plant Sci.* **13**, 983600 (2022).
29. Rajappa, S. et al. The translocation of a chloride channel from the Golgi to the plasma membrane helps plants adapt to salt stress. *Nat. Commun.* **15**, 3978–3992 (2024).
30. Lagacé, M. & Matton, D. P. Characterization of a WRKY transcription factor expressed in late torpedo-stage embryos of *Solanum chacoense*. *Planta* **219**, 185–189 (2004).

31. Sun, C. et al. A Novel WRKY transcription factor, SUSIBA2, participates in sugar signaling in barley by binding to the sugar-responsive elements of the *iso1* promoter. *Plant Cell* **15**, 2076–2092 (2003).
32. Hinderhofer, K. & Zentgraf, U. Identification of a transcription factor specifically expressed at the onset of leaf senescence. *Planta* **213**, 469–473 (2001).
33. Hollmann, J. et al. Identification of predominant genes involved in regulation and execution of senescence-associated nitrogen remobilization in flag leaves of field grown barley. *J. Exp. Bot.* **65**, 3963–3973 (2014).
34. Ulker, B. et al. The WRKY70 transcription factor of Arabidopsis influences both the plant senescence and defense signaling pathways. *Planta* **226**, 125–137 (2007).
35. Vatov, E. et al. Moderate DNA methylation changes associated with nitrogen remobilization and leaf senescence in Arabidopsis. *J. Exp. Bot.* **73**, 4733–4752 (2022).
36. Sachin, H. et al. WRKY1 mediates transcriptional regulation of light and nitrogen signaling pathways. *Plant Physiol.* **181**, 1371–1388 (2019).
37. Liao, H. S. et al. Glutamine induces lateral root initiation, stress responses, and disease resistance in Arabidopsis. *Plant Physiol.* **195**, 2289–2308 (2024).
38. Palmieri, M. C. et al. Nitric oxide-responsive genes and promoters in Arabidopsis thaliana: A bioinformatics approach. *J. Exp. Bot.* **59**, 177–186 (2008).
39. He, Y. et al. Programmed self-elimination of the *CRISPR/Cas9* construct greatly accelerates the isolation of edited and transgene-free rice plants. *Mol. Plant* **11**, 1210–1213 (2018).
40. Hiei, Y. et al. Efficient transformation of rice (*Oryza sativa* L.) mediated by *Agrobacterium* and sequence analysis of the boundaries of the T-DNA. *Plant J.* **6**, 271–282 (1994).
41. Li, S. et al. Modulating plant growth-metabolism coordination for sustainable agriculture. *Nature* **560**, 595–600 (2018).
42. Li, G. et al. Coordinated transcriptional regulation underlying the circadian clock in *Arabidopsis*. *Nat. Cell Biol.* **13**, 616–622 (2011).
43. Lin, R. et al. Transposase-derived transcription factors regulate light signaling in *Arabidopsis*. *Science* **318**, 1302–1305 (2007).
44. Wang, S. et al. The *OsSPL16-GW7* regulatory module determines grain shape and simultaneously improves rice yield and grain quality. *Nat. Genet* **47**, 949–954 (2015).
45. Ohta, M. et al. Repression domains of class II ERF transcriptional repressors share an essential motif for active repression. *Plant Cell* **13**, 1959–1968 (2001).
46. Hiratsu, K. et al. The SUPERMAN protein is an active repressor whose carboxy-terminal repression domain is required for the development of normal flowers. *Febs Lett.* **514**, 351–354 (2002).
47. Hao, Y. J. et al. Plant NAC-type transcription factor proteins contain a NARD domain for repression of transcriptional activation. *Planta* **232**, 1033–1043 (2010).
48. Chern, M. et al. A rice transient assay system identifies a novel domain in NRR required for interaction with NH1/OsNPR1 and inhibition of NH1-mediated transcriptional activation. *Plant Methods* **8**, 6–17 (2012).
49. Zheng, X. et al. Genomic signatures of domestication and adaptation during geographical expansions of rice cultivation. *Plant Biotech. J.* **20**, 16–18 (2022).
50. Li, H. & Durbin, R. Fast and accurate long-read alignment with Burrows-Wheeler transform. *Bioinformatics* **26**, 589–595 (2010).
51. Layer, R. M. et al. LUMPY: a probabilistic framework for structural variant discovery. *Genome Biol.* **15**, R84 (2014).
52. Liu, Y. et al. Genomic basis of geographical adaptation to soil nitrogen in rice. *Nature* **590**, 600–605 (2021).
53. Goldewijk, K. et al. Anthropogenic land use estimates for the Holocene - HYDE 3.2. *Earth Syst. Sci. Data* **9**, 927–953 (2017).

Acknowledgements

This research was supported by the National Key Research and Development Program of China (No. 2021YFF1000400 to Shan Li and S.W.), Jiangsu Province Government (No. BE2023331 to L.W.), National Natural Science Foundation of China (Nos. 32441065 and 32372121 to Shan Li), Jiangsu Funding Program for Excellent Postdoctoral Talent (No. 2024ZB460 to S.Z.), China Postdoctoral Science Foundation (No. GZB20240320 to S.Z.), Calleva Research Centre for Evolution and Human Sciences at Magdalen College, Oxford (to Z.J.), and Open Funds of the State Key Laboratory of Crop Genetics & Germplasm Enhancement and Utilization (ZW202302 to Z.J.).

Author contributions

Shan Li, S.Z., and Z.J. conceived and designed this study. S.Z. performed most of the experiments. S.Z., C.S., Y.Q., and Y.H. conducted map-based cloning. S.Z., M.H., S.K., X.L., Shunqi Li, Z.M, Y.Y., B.J., Y.T., and L.W. constructed transgenic rice plants and performed field and molecular experiments. W.J. performed bioinformatic analysis. S.W. provided SSSL lines. Shan Li and Z.J. wrote the manuscript. Z.J., Q.S., S.W., and Shan Li revised the manuscript. All authors discussed the results and contributed to the manuscript.

Competing interests

The authors declare no competing interests.

Additional information

Supplementary information The online version contains supplementary material available at https://doi.org/10.1038/s41467-025-56752-7.

Correspondence and requests for materials should be addressed to Shan Li.

Peer review information *Nature Communications* thanks Bipin Pandey and the other, anonymous, reviewer(s) for their contribution to the peer review of this work. A peer review file is available.